Hindawi
International Journal of Photoenergy
Volume 2022, Article ID 3727937, 15 pages
https://doi.org/10.1155/2022/3727937

Research Article

Effects of the Layered Distribution Pattern on the Gas Flow Resistance through the Bed with the Multisize Irregular Particle for the Waste Heat Recovery

Sizong Zhang [1,2]

[1]*School of Energy and Environmental Engineering, University of Science and Technology Beijing, Beijing 100083, China*
[2]*Beijing Key Laboratory of Energy Conservation and Emission Reduction for Metallurgical Industry, University of Science and Technology Beijing, Beijing 100083, China*

Correspondence should be addressed to Sizong Zhang; 513865909@qq.com

Received 15 April 2022; Accepted 2 June 2022; Published 21 June 2022

Academic Editor: Lixin Wang

The application of the sinter vertical cooling technology in the iron and steel industry is conducive to the realization of the double carbon in China. To reduce the energy consumption and improve the economy of the new process, the gas flow resistance in the sinter bed under the layered distribution pattern was experimentally studied. The gas flow resistance of most of the layered distribution modes is lower than that of the random distribution mode. Among all layered arrangement modes, the layered mode with the particle size increasing from the bottom-up has the lowest resistance, followed by the layered mode with the particle size decreasing from the bottom-up. These two modes ensure the feasibility of the application of the layered distribution pattern in the continuous production of the moving bed. Besides, increasing the number of layers benefits the reduction of the gas flow resistance, which has a more significant effect on the layered mode with the particle size increasing from the bottom-up. For the sinter mixture with the equivalent particle diameter of 11.45 mm, the gas resistance of the modes with the particle size increasing and decreasing from the bottom-up decreases by 11.71% and 8.26% with the layer number increasing from three to five, respectively. Also, the effect of the layered distribution pattern on the gas flow resistance progressively weakens with increasing the equivalent particle diameter. For the five-layer distribution mode with the particle size increasing from the bottom-up, the gas resistance decreases by 2.72% with the equivalent particle diameter increasing from 11.45 mm to 15.45 mm, while that decreases by 4.61% with the equivalent particle diameter increasing from 15.45 mm to 19.45 mm. What's more, the change of the equivalent particle diameter has a more significant influence on the layered mode with the particle size decreasing from the bottom-up. With the equivalent particle diameter increasing from 15.45 mm to 19.45 mm under the five-layer distribution pattern, the gas resistance of the layered mode with the particle size increasing from the bottom-up reduces by 4.61%, while that of the mode with the particle size decreasing from the bottom-up reduces by 7.38%.

1. Introduction

For realizing the green economic development system, China has put forward the targets of Carbon Peak in 2030 and Carbon Neutrality in 2060. Apart from vigorously developing the clean energy, including the solar energy, the breakthrough in the energy conversation and emission reduction technology of the traditional industry is a very important aspect, such as the iron and steel industry. The latest statistics show that the energy consumption of the iron and steel industry accounts for about 20% of the whole industry [1–4]. Among all processes, the energy consumption of the sintering process accounts for approximately 10~15% of the iron and steel industry, second only to the ironmaking process [5]. In the sintering process, the sensible heat of the sinter makes up about 70% of the waste heat resource. Therefore, improving the recovery rate of the sensible heat is of great significance for reducing the energy consumption of the sintering process and even the iron and steel industry. This would be a most promising method for China to realize the "double Carbon."

At present, the waste heat recovery of the high-temperature sinter is mainly through the annular cooling process. Since the air leakage rate of the annular cooler is as high as 35~50% and the cooling gas can only be heated to 150~380 °C, the recovery rate of the waste heat from the sinter is less than 30%. Given the shortcomings of the existing process, the vertical tank cooling process of the sinter has been newly proposed based on the coke dry quenching process [6, 7]. It is estimated that the vertical cooling process can increase the temperature of the cooling gas to 500~550 °C and increase the recovery rate from 30% to 80%.

The feasibility of the sinter vertical tank cooling process mainly depends on the gas-solid heat transfer and the gas flow resistance. The gas flow characteristic not only is the basis of the gas-solid heat transfer but also directly determines the pressure of the required fan and the power of the matching motor. For the sintering machine with the annual capacity of 4 million tons of the sinter, the heights of the sinter layer in the annular cooler and the vertical cooler are 0.8~1.5 m [5, 8–11] and 7~10 m [12, 13], respectively. Therefore, the gas flow resistance of the vertical cooler is much higher than that of the annular cooler. The excessive resistance not only makes it difficult for the gas to pass through the sinter layer but also reduces the efficiency of the gas-solid heat transfer and increases the energy consumption. Therefore, how to reduce the gas flow resistance is the key to the application of the sinter vertical tank cooling process.

In recent years, the relevant scholars have carried out some experimental researches on the resistance characteristic of the gas flow in the sinter bed [14–21]. Results showed that the gas flow resistance increased linearly with the bed height increasing [14], increased in a quadratic relationship with the increase of the gas velocity [14, 15], and decreased exponentially with the increase of the particle size and voidage [15]. Tian et al. [16] also found that the wall effect on the gas flow resistance can be ignored for $19 < D/d_p < 35$ (the ratio of the bed diameter D to the particle diameter d_p). However, the wall effect would lead to the reduction of the gas flow resistance for $7 < D/d_p < 19$. When the crushed sinter was added to the sinter mixture, the gas flow resistance in the bed would increase by 2~3 times [19]. In addition, the related studies on other particles are mainly concerned on the influences of the wall effect [22–24], particle shape [25–29], and particle size distribution [28–32] on the gas flow resistance. Therefore, there are few studies on how to reduce the gas flow resistance in the sinter bed.

In the actual production, the particle size of the sinter is nonuniform, but has a wide particle size distribution [17]. Therefore, the traditional distribution pattern, namely, the random distribution pattern, would cause the uneven distribution of the particle size and voidage in the sinter bed [33, 34]. The gas flow in the random bed is very disordered [35], leading to a sharp increase in the gas flow resistance and the uneven cooling of the high-temperature sinter. Besides, the gas flow in the packed bed with the double-size sinter was more disordered than that in the packed bed with the monosize sinter [18]. Compared with the particle bed of the wide particle size distribution, the gas flow in the particle bed of the narrow particle size distribution is more uniform, and the gas flow resistance is lower

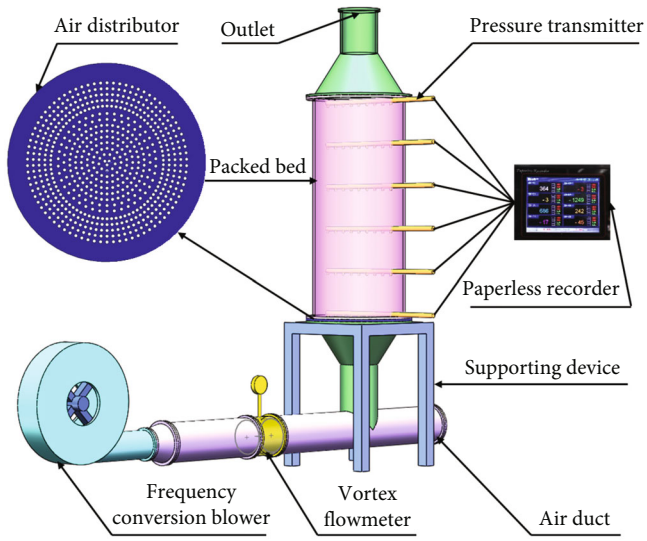

Figure 1: A sketch of the experimental apparatus for measuring the gas flow resistance in the sinter bed.

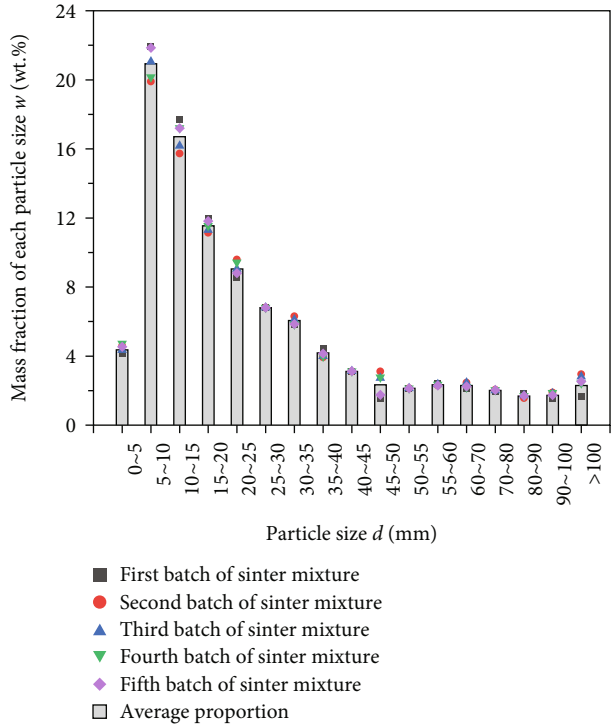

Figure 2: The original particle size distribution of sinter samples.

[36]. Based on the above reason, the layered distribution pattern based on the particle size is proposed [33, 34]; that is, the sinter mixture with the wide particle size distribution is divided into a variety of sinters with the narrow particle size distribution for the layered distribution. The numerical studies showed that the flow field and temperature distribution in the layered bed are relatively uniform [35]. Also, the recovery rate of the waste heat under the layered distribution pattern can be raised by about 14% compared with the random distribution pattern [33, 34].

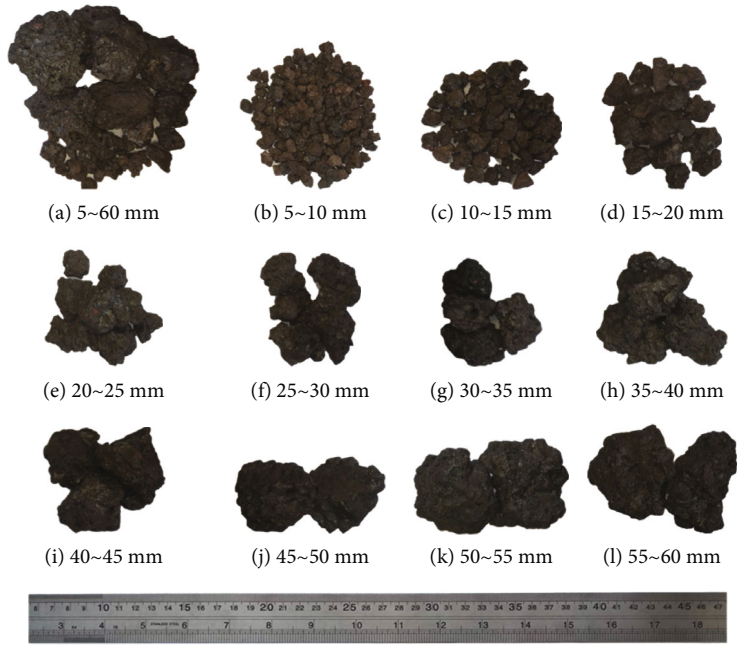

Figure 3: Photographs taken on the sinter of 5 ~60 mm: (a) the unsorted sinter mixture with the multisize; (b–l) 11 kinds of the sieved sinter with the monosize.

Table 1: Expressions of the measured and calculated method for characteristic parameters of sinter particles.

Characteristic parameter	Expression	Equation
Apparent density of the monosize sinter [17, 18]	$\rho_{a,s} = (m_1/m_3 - (m_2 - m_4))\rho_w$	(i)
Equivalent diameter of the monosize sinter [16, 17, 21]	$d_{p,s} = \sqrt[3]{6m_s/\pi\rho_{a,s}}$	(ii)
Apparent density of the sinter mixture [18]	$\rho_{a,m} = \sum_{i=1}^{n} w_i\rho_{a,si}$	(iii)
Equivalent diameter of the sinter mixture [29–31, 36]	$d_{p,m} = \sum_{i=1}^{n} w_i / \sum_{i=1}^{n} w_i/d_{p,si}$	(iv)
Bulk density [17, 18]	$\rho_b = (M_1 - M_2)/V$	(v)
Voidage [16–18, 21]	$\varepsilon = 1 - \rho_b/\rho_a$	(vi)

According to the above findings, the layered distribution pattern is beneficial to improve the uniformity of the gas flow and the sinter temperature in the packed bed. However, it is not known whether the uniform distribution of the gas flow is beneficial to reduce the gas flow resistance in the sinter bed. Therefore, from the viewpoint of reducing the energy consumption, the influence of the layered distribution pattern on the gas flow resistance is studied through experiments, thereby determining the optimal layered distribution mode.

2. Experimental Method

2.1. Experimental System. In this study, the experimental apparatus is constructed to measure the gas flow resistance in the sinter bed, as shown in Figure 1. As the main part of the experimental apparatus, the height and the inner diameter of the cylindrical bed are 1000 mm and 400 mm, respectively. The air distributor with the uniform openings is arranged at the bed bottom to obtain the uniform flow field in the cross-section. Six pressure taps are evenly arranged along the axial direction. For each tap, 9 measuring points are uniformly set along the radial direction to calculate the average pressure of the cross-section. The pressure transmitter (CGYL-202) with the length of 650 mm is selected to acquire the pressure information, the measured range and accuracy of which are 0~5 kPa and 0.5%, respectively. The frequency conversion blower (HRD 65FU-100/7.5) is selected to precisely control the gas flow rate. The vortex flowmeter with the compensation of the temperature and pressure (type: LUGB1315C-P3Z) is used to measure the gas flow rate under the standard condition (273.15 K and 101.325 kPa). The measured range and accuracy of the flowmeter are 150~2500 $Nm^3 \cdot h^{-1}$ and 1.0%, respectively.

2.2. Particle Characteristics of the Sinter. The sinter particles come from HBIS Group Hansteel Company in China. Before the test, five batches of original sinter mixtures are screened to obtain the particle size distribution, as shown in Figure 2.

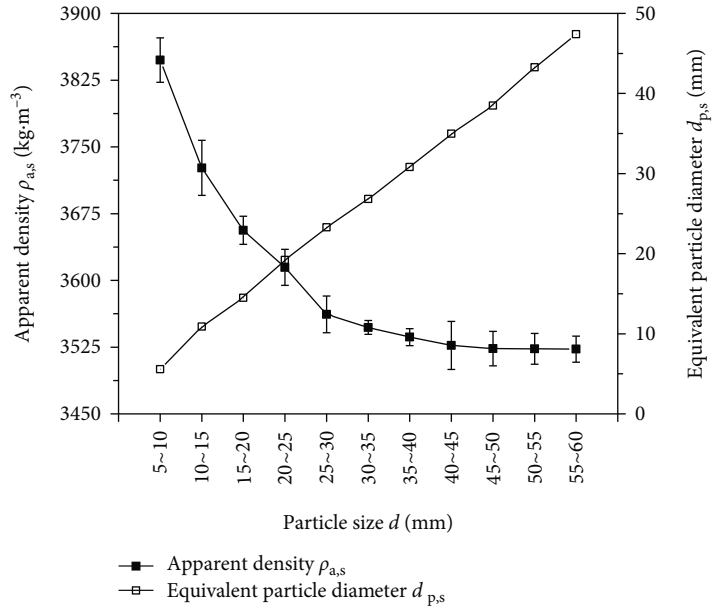

Figure 4: The apparent density $\rho_{a,s}$ and equivalent particle diameter $d_{p,s}$ of the monosize sinter under different particle sizes d.

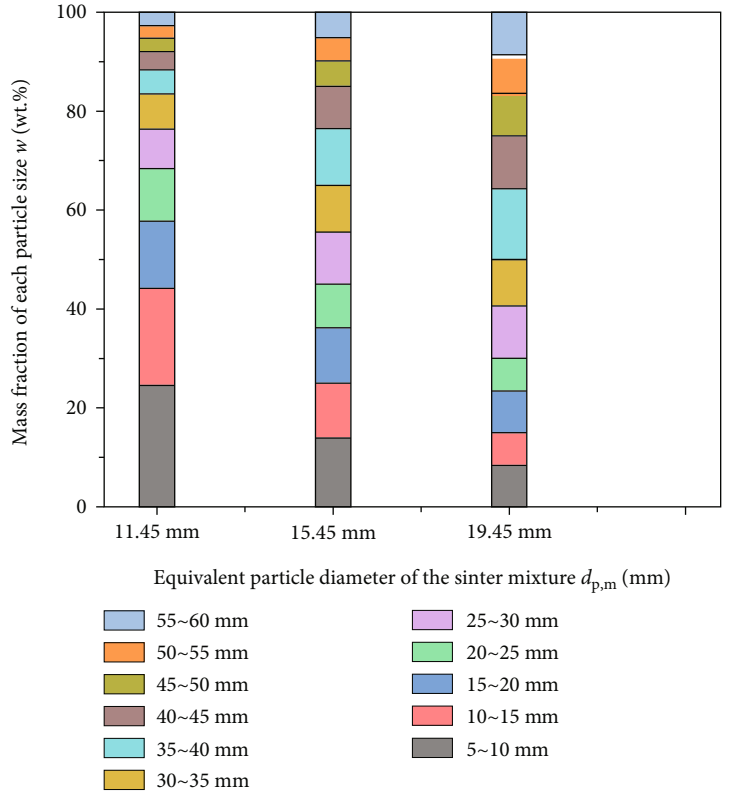

Figure 5: The particle size distribution of the three types of sinter mixtures.

It is observed that the particle size distribution among five batches of sinter mixtures is nearly consistent. Note that the sinter with the particle size range of 5~60 mm accounts for more than 85% of the total weight. Thus, they are taken for the test of the layered distribution, as shown in Figure 3.

To characterize the sinter of each monosize, the apparent density $\rho_{a,s}$ defined as Equation (i) in Table 1 is measured by the drainage method [17, 18], as shown in Figure 4. The equivalent particle diameter $d_{p,s}$ is calculated by Equation (ii) in Table 1 with the equal volume method [16, 17, 21].

Table 2: Characteristic parameters of the three kinds of sinter mixtures.

Equivalent particle diameter $d_{p,m}$ (mm)	Apparent density $\rho_{a,m}$ (kg·m^{-3})	Bulk density $\rho_{b,m}$ (kg·m^{-3})	Total height of the sinter bed L (cm)	Voidage ε
11.45	3676.09	1663.47	45.30	0.5475
15.45	3622.03	1581.00	47.11	0.5635
19.45	3589.73	1512.95	49.23	0.5785

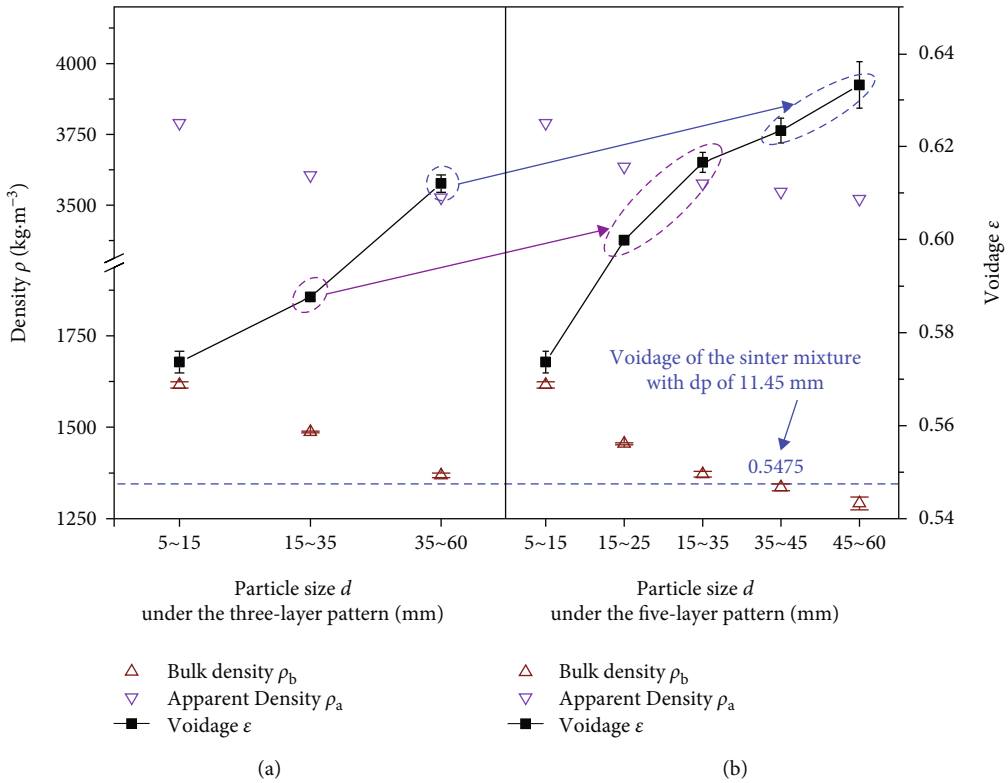

Figure 6: Characteristic parameters of the sinter in each particle size range under the three-layer pattern (a) and the five-layer pattern (b).

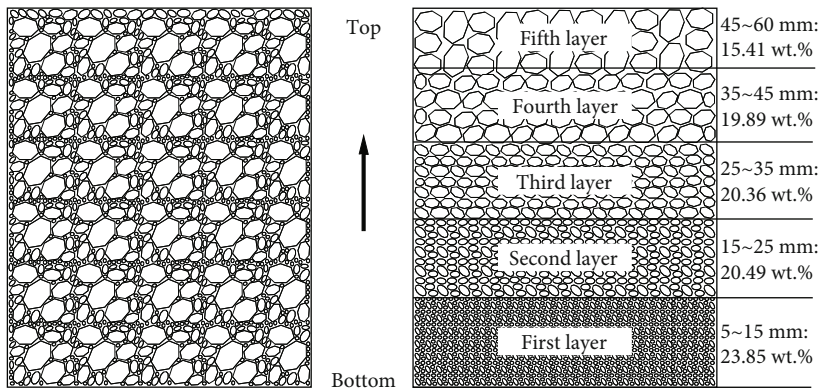

Figure 7: The schematic diagram of the distribution mode: (a) the random distribution mode; (b) the five-layer arrangement mode with the particle size increasing from the bottom-up (i.e., mode 1 in Table 4).

Table 3: All three-layer arrangement modes for the sinter mixture with the equivalent particle diameter of 11.45 mm.

Mode of the layered arrangement	Particle size range of the sinter in each layer d (mm) Bed bottom→bed top			Total height of the sinter layer L (cm)	Ratio of the resistance increase S_k (%)
	First layer	Second layer	Third layer		
0	Random distribution mode (control condition)			45.30	/
1	5~15	15~35	35~60	47.02	-13.99
2	5~15	35~60	15~35	46.54	-6.92
3	15~35	5~15	35~60	46.65	-9.65
4	15~35	35~60	5~15	46.14	-10.95
5	35~60	5~15	15~35	46.03	3.93
6	35~60	15~35	5~15	46.92	-11.89

Table 4: All five-layer arrangement modes for the sinter mixture with the equivalent particle diameter of 11.45 mm.

Mode of the layered arrangement	Particle size range of the sinter in each layer d (mm) Bed bottom→bed top					Total height of the sinter layer L (cm)	Ratio of the resistance increase S_k (%)
	First layer	Second layer	Third layer	Fourth layer	Fifth layer		
0	Random distribution mode (control condition)					45.30	/
1	5~15	15~25	25~35	35~45	45~60	47.36	-25.70
2	15~25	25~35	35~45	45~60	5~15	46.25	-0.56
3	25~35	35~45	45~60	5~15	15~25	47.12	-14.99
4	35~45	45~60	5~15	15~25	25~35	47.27	-10.19
5	45~60	5~15	15~25	25~35	35~45	46.74	-2.93
6	5~15	25~35	45~60	15~25	35~45	46.70	-3.32
7	15~25	35~45	5~15	25~35	45~60	46.58	2.95
8	25~35	45~60	15~25	35~45	5~15	46.37	-2.04
9	35~45	5~15	25~35	45~60	15~25	46.23	-4.63
10	45~60	15~25	35~45	5~15	25~35	45.85	-5.13
11	5~15	35~45	15~25	45~60	25~35	45.25	-1.75
12	15~25	45~60	25~35	5~15	35~45	45.51	-7.09
13	25~35	5~15	35~45	15~25	45~60	46.71	-1.52
14	35~45	15~25	45~60	25~35	5~15	46.16	4.85
15	45~60	25~35	5~15	35~45	15~25	45.84	3.99
16	5~15	45~60	35~45	25~35	15~25	46.02	3.24
17	15~25	5~15	45~60	35~45	25~35	46.04	1.74
18	25~35	15~25	5~15	45~60	35~45	46.22	-10.90
19	35~45	25~35	15~25	5~15	45~60	46.01	-3.91
20	45~60	35~45	25~35	15~25	5~15	46.62	-20.15

Table 5: Summary of the relative uncertainty of parameters in this study.

Parameter	Symbol	Uncertainty (%)	Parameter	Symbol	Uncertainty (%)
Equivalent particle diameter	d_p	1.51	Gas velocity	u_g	1.00
Apparent density	ρ_a	1.42	Voidage	ε	1.81
Bulk density	ρ_b	1.12	Gas resistance	ΔP	0.50

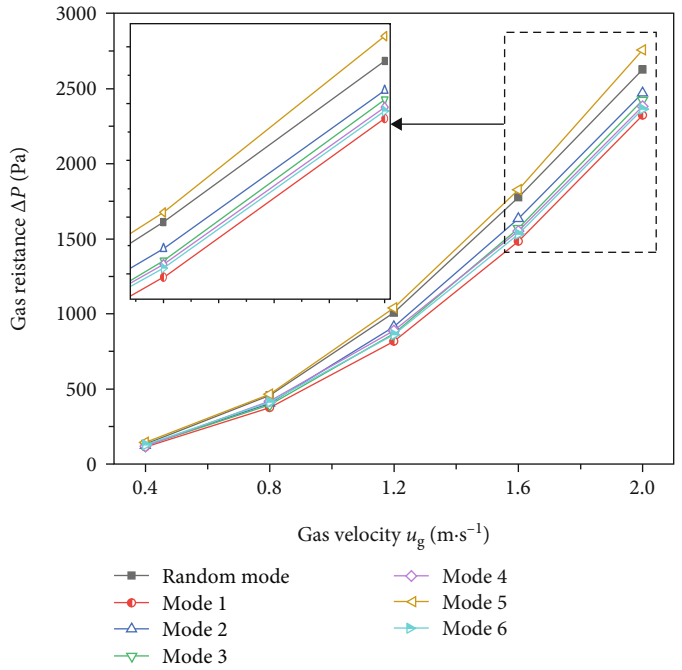

Figure 8: The change of the gas resistance ΔP with the gas velocity u_g under the three-layer layered arrangement modes and the random distribution mode for the sinter mixture with the equivalent particle diameter of 11.45 mm.

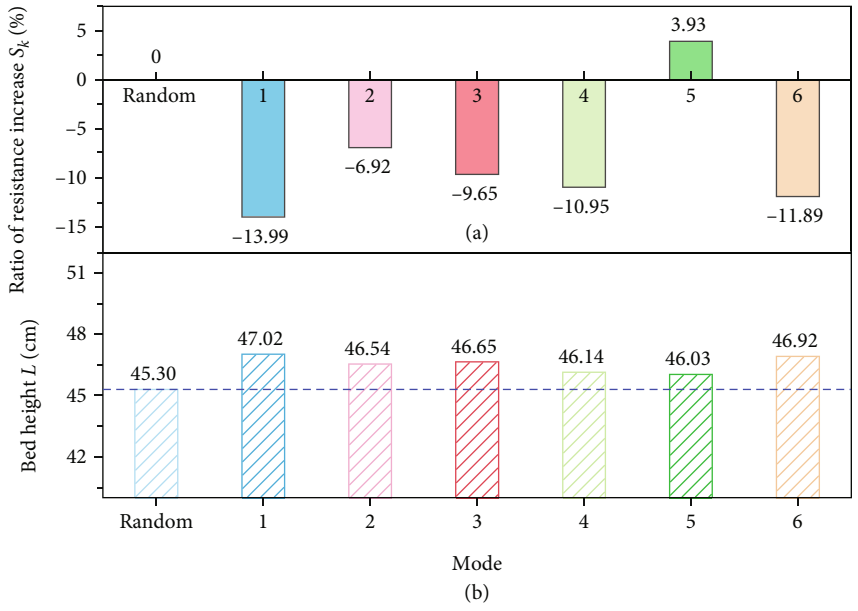

Figure 9: The ratio of the resistance increase S_k (a) and the total height of the sinter bed L (b) under different three-layer arrangement modes for the sinter mixture with the equivalent particle diameter of 11.45 mm.

For the multisize sinter mixture composed of a variety of the monosize sinter, the apparent density $\rho_{a,m}$ and equivalent particle diameter $d_{p,m}$ can be calculated by Equation (iii) in Table 1 [18] with the weighted method and Equation (iv) in Table 1 with the weighted harmonic mean method [29–31, 36], respectively. For multisize sinter mixtures and monosize sinters, the bulk density ρ_b can be measured by the weighing method of Equation (v) in Table 1 [17, 18]. The bed voidage ε can be calculated by Equation (vi) in Table 1 [16–18, 21].

To study the influence of the particle size distribution on the gas flow resistance under the layered distribution

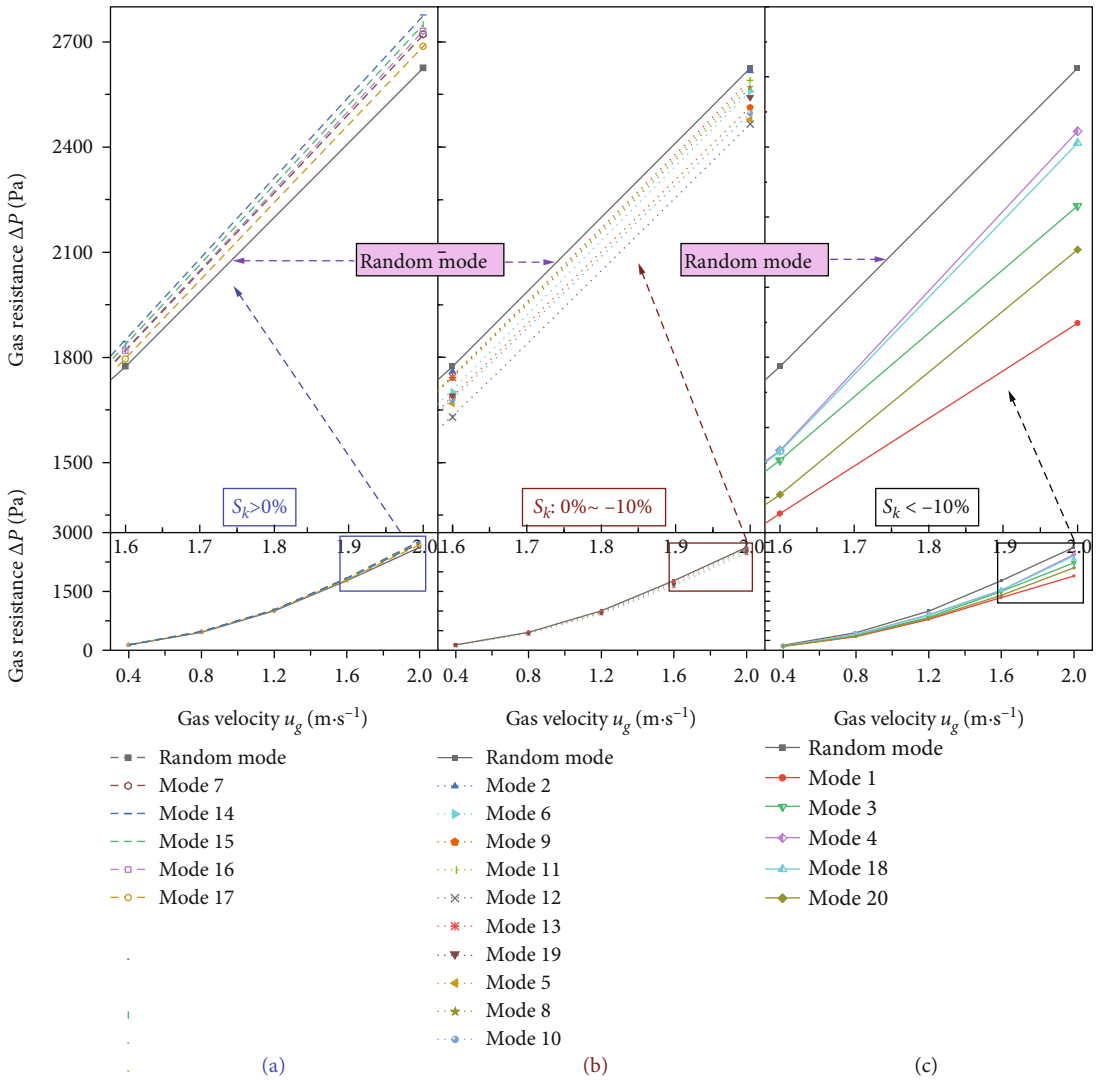

FIGURE 10: The comparison of the gas flow resistance ΔP between the five-layer layered mode and the random distribution mode based on the sinter mixture with the equivalent particle diameter of 11.45 mm: (a) the ratio of the resistance increase $S_k > 0\%$; (b) the ratio of the resistance increase S_k: 0%~-10%; (c) the ratio of the resistance increase S_k <-10%.

pattern, three types of sinter mixtures are designed, as shown in Figure 5. The equivalent particle diameters $d_{p,m}$ of the three kinds of sinter mixtures are 11.45 mm, 15.45 mm, and 19.45 mm, respectively. To ensure the comparability of experimental results, the mass of the three kinds of sinter mixtures is the same, which is 94.30 kg. The characteristic parameters of the sinter mixture obtained by the above methods are shown in Table 2.

To analyze the effect of the layer number on the gas flow resistance, two types of the layered distribution patterns are studied. The first type is divided into three layers, which is composed of the three kinds of sinters with the particle size of 5~15 mm, 15~35 mm, and 35~60 mm. The second type is divided into five layers, which contains the five kinds of sinters with the particle size of 5~15 mm, 15~25 mm, 25~35 mm, 35~45 mm, and 45~60 mm. The bulk density ρ_b, apparent density ρ_a, and voidage ε of the sinter of each particle size are measured by means of the above methods, as shown in Figure 6.

To analyze the effect of the gas velocity u_g, the gas resistance in the layered bed is measured under the five kinds of gas velocities, namely, 0.4, 0.8, 1.2, 1.6, and 2.0 m·s^{-1}. The conventional random distribution pattern is also studied as the control experiment, as shown in Figure 7. To study the effect of the layered arrangement mode, the gas resistance in the bed of the sinter mixture with the equivalent particle diameter of 11.45 mm is measured under 6 kinds of three-layer arrangement modes and 20 kinds of five-layer arrangement modes based on the orthogonal design, as shown in Tables 3 and 4, respectively. Tables also list the ratio of the resistance increase S_k for different layered arrangement modes compared with the random distribution mode, which is defined as follows:

$$S_k = \frac{1}{n}\sum_{i=1}^{n=5}\frac{\Delta P_k^i - \Delta P_r^i}{\Delta P_r^i}, \quad (1)$$

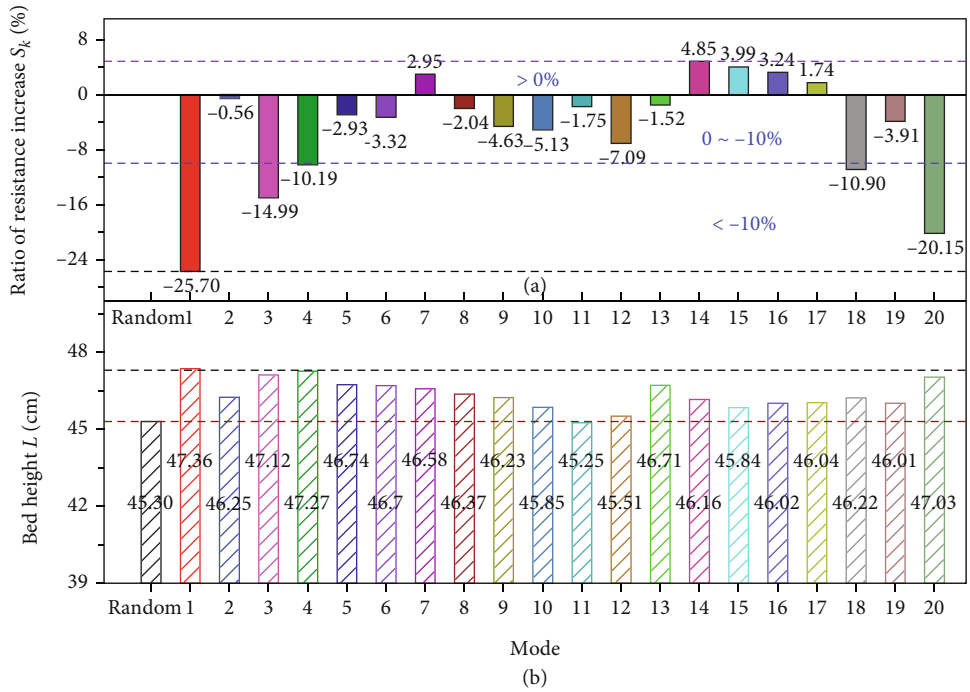

FIGURE 11: The ratio of the resistance increase S_k (a) and the total height of the sinter bed L (b) under different five-layer layered arrangement modes for the sinter mixture with the equivalent particle diameter of 11.45 mm.

where S_k is the ratio of the resistance increase of the k-th layered arrangement mode; ΔP_r^i and ΔP_k^i represent the gas resistance of the i-th gas velocity under the random distribution mode and the k-th layered arrangement mode, respectively; and i is the condition of the i-th gas velocity.

2.3. Uncertainty Analysis. The uncertainty analysis of parameters is calculated by the theory of the error transfer [21, 37–39]. Suppose the relationship between the parameter y and k variables is as follows:

$$y = f(x_1, x_2, x_3, \cdots, x_k), \tag{2}$$

where $x_1, x_2, x_3, \cdots, x_k$ are k independent variables.

Then the absolute uncertainty of y (Δy) can be calculated according to the absolute uncertainty of each independent variable ($\Delta x_1, \Delta x_2, \Delta x_3, \cdots, \Delta x_k$) as follows:

$$\Delta y = \sqrt{\sum_{j=1}^{k} \left(\frac{\partial f}{\partial x_j} \Delta x_j \right)^2}. \tag{3}$$

Therefore, the relative uncertainty of y is expressed as

$$\frac{\Delta y}{y} = \sqrt{\sum_{j=1}^{k} \left(\frac{\Delta x_j}{x_j} \right)^2}. \tag{4}$$

The relative uncertainty of each parameter is shown in Table 5.

3. Experimental Results and Discussion

3.1. Analysis of the Three-Layer Arrangement Mode. Figure 8 shows the change of the gas flow resistance (ΔP) with the gas velocity (u_g) under the three-layer layered mode and the random mode for the sinter mixture with the equivalent particle diameter of 11.45 mm. It can be observed that ΔP increases in a quadratic relationship with the increase of u_g. With the increase of u_g, the collision between the gas and sinter particles will intensify. Therefore, the turbulent degree of the gas flow increases, which makes the gas resistance increase [14].

Based on the data in Figure 8, the ratio of the resistance increase S_k under different three-layer arrangement modes is calculated, as shown in Figure 9(a). It can be found that the gas flow resistance (ΔP) of most of the layered arrangement modes is lower than that of the random distribution mode. On the one hand, the mixing degree of sinters under the layered distribution mode is lower than that of the random distribution mode. Therefore, Figure 6(a) shows that the voidage of each layer under the layered distribution mode is larger than that of the random distribution mode. This reduces the viscous resistance and the inertial resistance of the gas flow [14, 40]. On the other hand, the interval width of the particle size of the sinter in each layer under the layered distribution mode is narrower than that of the random distribution mode. The voidage distribution along the radial direction under the layered bed is more uniform, which reduces the disorder of the gas flow [35, 36].

Also, it can be seen from Figure 9(a) that the gas flow resistance of mode 1 and mode 6 is the smallest, which is 13.99% and 11.89% lower than that of the random distribution mode,

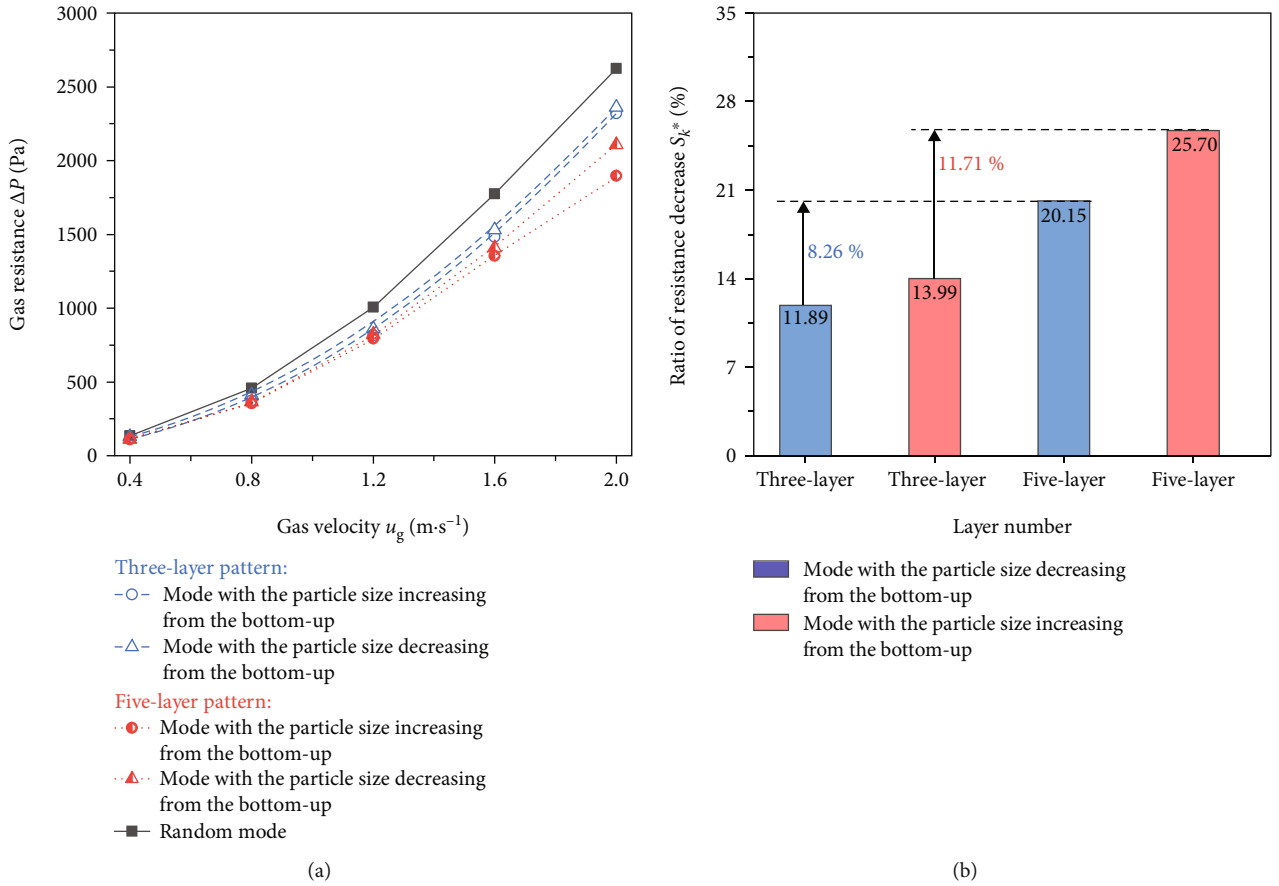

Figure 12: The effect of the layer number on the gas flow resistance of the sinter mixture with the equivalent particle diameter of 11.45 mm: (a) the comparison of the gas flow resistance ΔP between two three-layer modes and two five-layer modes; (b) the comparison of the ratio of the resistance decrease S_k^* between the two three-layer models and two five-layer models.

respectively. It can be seen from Table 3 that mode 1 and mode 6 are the arrangement modes with the particle size increasing and decreasing from the bed bottom to the bed top, respectively. As can be seen from Figure 9(b), the bed height of these two modes is the highest. This indicates that the mixing degree of particles at the interface of adjacent layers is the lowest due to the continuous change of the particle size. Therefore, the disorder degree of the gas flow through the bed and the local resistance at the interface are relatively the lowest. Unexpectedly, the gas resistance of mode 5 is 3.93% higher than that of the random distribution mode. However, the ratio of the resistance increase is very small. Therefore, the gas flow resistance in the packed bed under the five-layer layered distribution pattern is further studied.

3.2. Analysis of the Five-Layer Arrangement Model. As shown in Figure 10 based on the sinter mixture with the equivalent particle diameter of 11.45 mm, the gas flow resistance ΔP is compared between all five-layer layered modes and the random distribution mode. Notably, Figure 10(a) shows that there are indeed several layered modes, ΔP of which is higher than that of the random distribution mode.

Based on the ratio of the resistance increase S_k of Figure 11(a), all layered modes can be divided into three categories, namely, $S_k > 0\%$, $0 > S_k > -10\%$, and $S_k < -10\%$. According to Figure 11(b), the average bed heights of the layered mode of $S_k > 0\%$, $0 > S_k > -10\%$, and $S_k < -10\%$ are 45.88 cm, 46.41 cm, and 46.88 cm, respectively. For the same batch of the sinter mixture, the bed voidage reduces with the decrease of the bed height. The lower the bed voidage, the greater the gas flow resistance. Besides, it can be seen from Table 4 that the particle size of the sinter between adjacent layers changes greatly under the five layered modes of $S_k > 0\%$. The great change of the particle size between adjacent layers would produce two factors to increase the resistance. On the one hand, the mixing degree of sinter particles between adjacent layers increases. This makes the uniformity of the voidage distribution along the radial distribution reduce, which increases the turbulent degree of the gas flow. On the other hand, the change range of the voidage along the axial direction at the interface of adjacent layers increases. This makes the gas flow expand or contract abruptly at the interface, increasing the local resistance. For the layered mode of $S_k < -10\%$, the particle size of the sinter between adjacent layers changes little, which basically shows the continuous increase or the continuous decrease. The mixing degree of the sinter between adjacent layers reduces. This not only improves the uniformity of the voidage

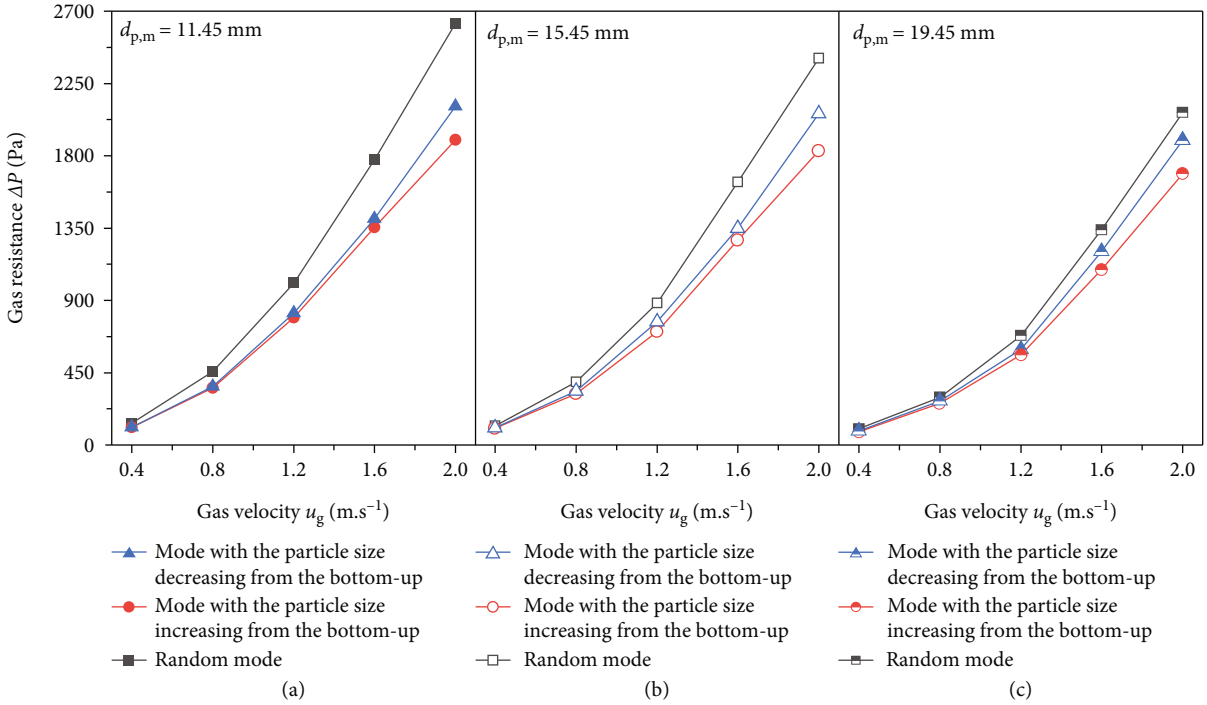

FIGURE 13: The comparison of the gas flow resistance (ΔP) between the random distribution mode and two kinds of five-layer distribution modes under the three kinds of sinter mixtures: (a) $d_{p,m}$ = 11.45 mm; (b) $d_{p,m}$ = 15.45 mm; (c) $d_{p,m}$ = 19.45 mm.

distribution along the radial direction, but also reduces the variation range of the axial voidage at the interface. Therefore, the gas can flow evenly through the sinter layer, which reduces the turbulent degree and the local resistance of the gas flow.

As can be seen from Figure 11(a) for the five-layer distribution pattern, the gas flow resistance of modes with the particle size increasing and decreasing from the bottom-up (i.e., modes 1 and 20) is also the lowest, which is 25.70% and 20.15% lower than that of the random distribution mode, respectively. For the layered distribution pattern, the layered mode with the particle size increasing from the bottom-up has the smallest resistance, followed by the mode with the particle size decreasing from the bottom-up. Compared with the layered mode with the particle size increasing from the bottom-up, the small-size sinter in the upper layer can be easily filled into gaps between the large-size sinters in the lower layer for the mode with the particle size decreasing from the bottom-up. Therefore, the packing structure of the mode with the particle size decreasing from the bottom-up is more complex, intensifying the disorder and resistance of the gas flow.

3.3. Effect of the Layer Number. Figure 12 illustrates the effect of the layer number on the gas flow resistance. In Figure 12(b), S_k^* is defined as the ratio of the resistance decrease of the layered distribution mode compared to the random distribution mode. As seen from Figure 12(a), the gas flow resistance of the three-layer bed is higher than that of the five-layer packed bed under two kinds of layered modes with the particle size increasing and decreasing from the bottom-up. Besides, Figure 12(b) indicates that the gas flow resistance of the mode with the particle size decreasing from the bottom-up declines by 8.26% with the layer number increasing from three to five, while that decreases by 11.71% for the mode with the particle size increasing from the bottom-up. Therefore, the increase of the layer number is not only conducive to further reduce the gas flow resistance, but also has a more significant impact on the mode with the particle size increasing from the bottom-up. This can be attributed to the following two aspects. On the one hand, the sinter with the particle size of 15~35 mm under the three-layer distribution pattern is composed of the sinter with the particle size of 15~25 mm and 25~35 mm under the five-layer distribution pattern. And the sinter with the particle size of 35~60 mm consists of the sinter with the particle size of 35~45 mm and 45~60 mm. Therefore, the packing structure in the three-layer packed bed is more complex. The distribution homogeneity of the voidage and particle size along the radial direction reduces, which increases the disorder degree of the gas flow [36]. On the other hand, Figure 6 shows that the bed voidage of the sinter with the particle size of 15~25 and 25~35 mm is bigger than that of the sinter with the particle size of 15~35 mm. And the voidage of the sinter with the particle size of 35~45 and 45~60 mm is also bigger than that of the sinter of with the particle size of 35~60 mm. Therefore, the overall voidage of the three-layer packed bed is smaller, leading to an increase in the gas flow resistance [40].

3.4. Effect of the Equivalent Particle Diameter. Figure 13 compares the gas flow resistance of the three types of sinter mixtures under the three kinds of distribution modes. The gas flow resistance of the three modes decreases with the

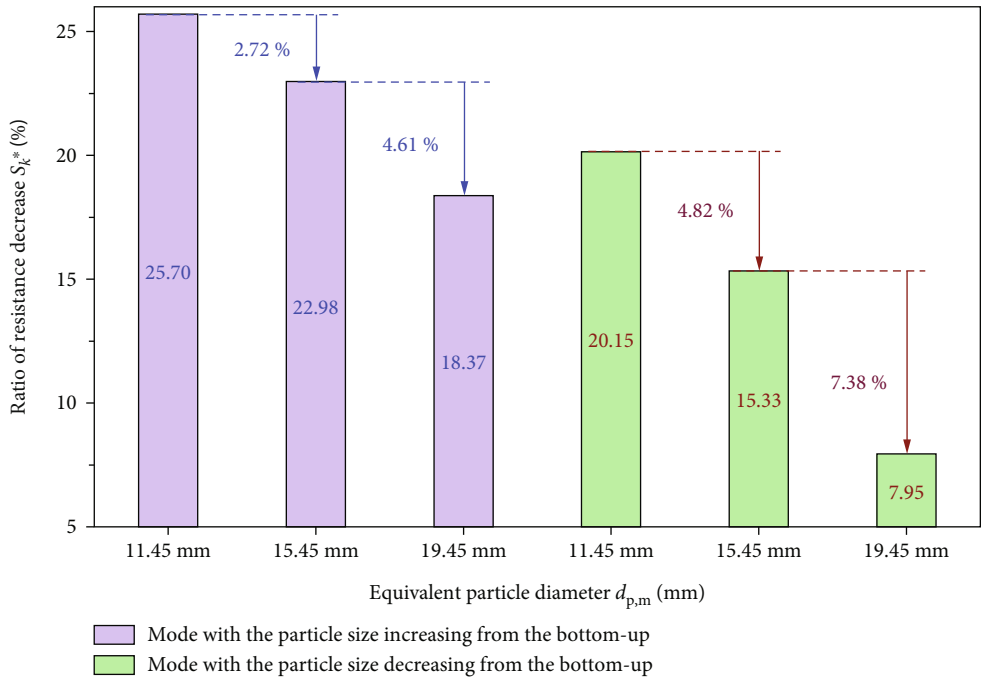

FIGURE 14: Effect of the equivalent particle diameter $d_{p,m}$ on the ratio of the resistance decrease S_k^* under the two five-layer layered arrangement modes.

increase of the equivalent particle diameter $d_{p,m}$. Table 2 shows that the overall voidage of the sinter mixture increases with the increase of $d_{p,m}$. This leads to the reduction of the flow instability and specific surface area, decreasing the inertial resistance and viscous resistance.

Based on the data in Figure 13, the ratio of the resistance decrease S_k^* of the two five-layer modes under the three kinds of equivalent particle diameters $d_{p,m}$ is calculated, as shown in Figure 14. The ratio of the resistance decrease S_k^* under two kinds of layered modes decreases with the increase of the equivalent particle diameter $d_{p,m}$. Moreover, S_k^* of the mode with the particle size increasing from the bottom-up decreases by 2.72% with $d_{p,m}$ increasing from 11.45 mm to 15.45 mm, while that decreases by 4.61% with $d_{p,m}$ increasing from 15.45 mm to 19.45 mm. This indicates that the effect of the layered distribution pattern on the resistance reduction progressively weakens with the increase of $d_{p,m}$. It can be seen from Figure 5 that the proportion of the small-size sinter and the large-size sinter would decrease and increase when the equivalent particle diameter increases, respectively. Therefore, it is easier to form large gaps between particles. For the layered distribution mode, the possibility of the small particle in adjacent layers filling into gaps between large particles under the action of the gravity increases. The nonuniformity of the voidage distribution along the radial direction increases, which makes the layered mode close to the random mode to some extent. Therefore, the increase of the equivalent particle diameter weakens the effect of the layered distribution mode on the disorder degree of the gas flow.

With the increase of the equivalent diameter $d_{p,m}$, Figure 14 also shows that the change range of the ratio of the resistance decrease S_k^* for the mode with the particle size decreasing from the bottom-up is greater than that for the mode with the particle size increasing from the bottom-up. When the equivalent particle diameter $d_{p,m}$ increases from 15.45 mm to 19.45 mm, S_k^* of the mode with the particle size increasing from the bottom-up decreases by 4.61%, while that of the mode with the particle size decreasing from the bottom-up decreases by 7.38%. Hence, the increase of the equivalent particle diameter has a greater influence on the mode with the particle size decreasing from the bottom-up. For the layered mode with the particle size increasing from the bottom-up, the size of the gap between sinters in the lower layer is smaller than that of the sinter in the upper layer. The sinter particles in the upper layer are difficult to fill into gaps in the lower layer. Therefore, the packing structure of the sinters is almost unchanged. The increase of the equivalent particle diameter has little effect on the bed structure of the mode with the particle size increasing from the bottom-up. For the mode with the particle size decreasing from the bottom-up, the probability of the small-size sinter in the upper layer filling into gaps between the large particles in the lower layer increases gradually with the increase of the equivalent particle diameter $d_{p,m}$. The packing structure of the mode with the particle size decreasing from the bottom-up is more similar to that of the random mode. Therefore, the gas resistance of the mode with the particle size decreasing from the bottom-up is more significantly affected by the change of the equivalent particle diameter.

4. Conclusions

The sinter vertical cooling technology is conducive to the realization of the double carbon in the iron and steel industry. To reduce the energy consumption of the new process, the gas flow resistance in the sinter bed under the layered distribution pattern was experimentally studied. The effects of three factors, namely, the layered arrangement mode, the layer number, and the equivalent particle diameter, are carefully discussed.

The results show that the gas flow resistance of most of the layered distribution modes is lower than that of the random distribution mode. This indicates that the application of the layered distribution pattern is beneficial to reduce the gas resistance in the sinter bed. Among all layered modes, the layered mode with the particle size increasing from the bottom-up has the lowest resistance, followed by the mode with the particle size decreasing from the bottom-up. Since the operation state of the sinter vertical cooling process is continuous, these two modes ensure the feasibility of the application of the layered distribution pattern. Besides, the increase of the layer number not only is conducive to reduce the gas resistance but also has a more significant impact on the layered mode with the particle size increasing from the bottom-up. Moreover, the effect of the layered distribution pattern on the gas flow resistance progressively weakens with the increase of the equivalent particle diameter. What's more, the mode with the particle size decreasing from the bottom-up is more significantly affected by the equivalent particle diameter.

This work not only is helpful to understand the effect of the layered distribution pattern on the gas resistance characteristic but also lays a foundation for the application of the layered distribution pattern in the moving bed. However, the bed structure and the mechanism of the gas flow under the layered distribution pattern are still unclear, which is an important research direction in the future.

Nomenclature

D: Diameter of the packed bed (m)
d: Particle size of the sinter (m)
d_p: Equivalent particle diameter of the sinter (m)
$d_{p,s}$: Equivalent particle diameter of the monosize sinter (m)
$d_{p,si}$: Equivalent particle diameter of a certain monosize sinter in the sinter mixture (m)
$d_{p,m}$: Equivalent particle diameter of the sinter mixture (m)
L: Height of the sinter bed (m)
ρ_a: Apparent density of sinter (kg·m^{-3})
m_1: Mass of the dry sinter (kg)
m_2: Mass of the sinter and test basket in water (kg)
m_3: Mass of the wet sinter (kg)
m_4: Mass of the test basket in water (kg)
M_1: Mass of a batch of the sinter and test container (kg)
M_2: Mass of the test container (kg)
ρ_w: Density of the water (kg·m^{-3})
m_s: Mean mass of the single sinter (kg)
$\rho_{a,m}$: Apparent density of the sinter mixture (kg·m^{-3})
$\rho_{a,s}$: Apparent density of the monosize sinter (kg·m^{-3})
$\rho_{a,si}$: Apparent density of a certain monosize sinter in the sinter mixture (kg·m^{-3})
ρ_b: Bulk density of the sinter (kg·m^{-3})
u_g: Gas velocity under the standard condition (m·s^{-1})
V: Volume of the test container (m^3)
w: Mass fraction of the sinter (wt.%)
w_i: Mass fraction of a certain monosize sinter in the sinter mixture (wt.%)
ΔP: Gas flow resistance in the sinter packed bed (Pa)
ΔP_r^i: The gas flow resistance of a certain gas velocity under the random distribution mode (Pa)
ΔP_k^i: Gas flow resistance of a certain gas velocity under a certain layered arrangement mode (Pa)
S_k: Ratio of the resistance increase of a certain layered arrangement mode (%)
S_k^*: The ratio of the resistance decrease of a certain layered arrangement mode (%)

Greeks

ρ: Density (kg·m^{-3})
ε: Voidage

Subscripts

p: Particle
w: Water
g: Gas

Data Availability

The data used to support the findings of this study are included within the article.

Conflicts of Interest

The authors declare that they have no known competing financial interests or personal relationships that could have appeared to influence the work reported in this paper.

Acknowledgments

This work is supported by Basic and Applied Basic Research Fund of Guangdong (2019A1515110743).

References

[1] Y. Li and L. Zhu, "Cost of energy saving and CO_2 emissions reduction in China's iron and steel sector," *Applied Energy*, vol. 130, pp. 603–616, 2014.

[2] Q. Xu, K. Wang, Z. W. Zou et al., "A new type of two-supply, one-return, triple pipe-structured heat loss model based on a low temperature district heating system," *Energy*, vol. 218, article 119569, 2021.

[3] Q. Xu, Z. W. Zou, Y. S. Chen et al., "Performance of a novel-type of heat flue in a coke oven based on high-temperature and low-oxygen diffusion combustion technology," *Fuel*, vol. 267, article 117160, 2020.

[4] Q. Xu, L. Liu, J. X. Feng et al., "A comparative investigation on the effect of different nanofluids on the thermal performance

of two-phase closed thermosyphon," *International Journal of Heat and Mass Transfer*, vol. 149, article 119189, 2020.

[5] X. H. Zhang, Z. Chen, J. Y. Zhang, P. X. Ding, and J. M. Zhou, "Simulation and optimization of waste heat recovery in sinter cooling process," *Applied Thermal Engineering*, vol. 54, no. 1, pp. 7–15, 2013.

[6] Y. H. Feng, X. X. Zhang, Q. Yu et al., "Experimental and numerical investigations of coke descending behavior in a coke dry quenching cooling shaft," *Applied Thermal Engineering*, vol. 28, no. 11-12, pp. 1485–1490, 2008.

[7] K. Sun, C. Tseng, D. S. Wong et al., "Model predictive control for improving waste heat recovery in coke dry quenching processes," *Energy*, vol. 80, pp. 275–283, 2015.

[8] Y. Liu, J. Yang, J. Wang, Z. L. Cheng, and Q. W. Wang, "Energy and exergy analysis for waste heat cascade utilization in sinter cooling bed," *Energy*, vol. 67, pp. 370–380, 2014.

[9] H. J. Feng, L. G. Chen, X. Liu, Z. H. Xie, and F. R. Sun, "Constructal optimization of a sinter cooling process based on exergy output maximization," *Applied Thermal Engineering*, vol. 96, pp. 161–166, 2016.

[10] X. Shen, L. G. Chen, S. J. Xia, and F. R. Sun, "Numerical simulation and analyses for sinter cooling process with convective and radiative heat transfer," *International Journal of Energy and Environment*, vol. 7, no. 4, pp. 303–316, 2016.

[11] S. Zhang, L. Zhao, J. S. Feng, X. F. Luo, and H. Dong, "Parameter optimization of gas-solid heat transfer process in sinter packed bed based on further exergy analysis," *Chemical Engineering Research and Design*, vol. 146, pp. 499–508, 2019.

[12] J. S. Feng, H. Dong, J. Y. Gao, H. Z. Li, and J. Y. Liu, "Numerical investigation of gas-solid heat transfer process in vertical tank for sinter waste heat recovery," *Applied Thermal Engineering*, vol. 107, pp. 135–143, 2016.

[13] J. S. Feng, S. Zhang, H. Dong, and G. Pei, "Effect of gas inlet parameters on exergy transfer performance of sinter cooling process in vertical moving bed," *Applied Thermal Engineering*, vol. 152, pp. 126–134, 2019.

[14] J. S. Feng, H. Dong, and H. D. Dong, "Modification of Ergun's correlation in vertical tank for sinter waste heat recovery," *Powder Technology*, vol. 280, pp. 89–93, 2015.

[15] J. S. Feng, H. Dong, J. Y. Liu, K. Liang, and J. Y. Gao, "Experimental study of gas flow characteristics in vertical tank for sinter waste heat recovery," *Applied Thermal Engineering*, vol. 91, pp. 73–79, 2015.

[16] F. Y. Tian, L. F. Huang, L. W. Fan, H. L. Qian, and Z. T. Yu, "Wall effects on the pressure drop in packed beds of irregularly shaped sintered ore particles," *Powder Technology*, vol. 301, pp. 1284–1293, 2016.

[17] F. Y. Tian, L. F. Huang, L. W. Fan et al., "Pressure drop in a packed bed with sintered ore particles as applied to sinter coolers with a novel vertically arranged design for waste heat recovery," *Journal of Zhejiang University-Science A (Applied Physics & Engineering)*, vol. 17, no. 2, pp. 89–100, 2016.

[18] F. Y. Tian, L. F. Huang, L. W. Fan, Z. T. Yu, and Y. C. Hu, "Experimental study on pressure drop of packed beds with binary sintered ore particle mixtures," *Journal of Zhejiang University (Engineering Science)*, vol. 50, no. 11, pp. 2077–2086, 2016.

[19] L. S. Pan, X. L. Wei, Y. Peng, X. B. Shi, and H. L. Liu, "Experimental study on convection heat transfer and air drag in sinter layer," *Journal of Central South University*, vol. 22, no. 7, pp. 2841–2848, 2015.

[20] J. S. Feng, S. Zhang, H. Dong, and G. Pei, "Frictional pressure drop characteristics of air flow through sinter bed layer in vertical tank," *Powder Technology*, vol. 344, pp. 177–182, 2019.

[21] Y. Liu, J. Y. Wang, Z. L. Cheng, J. Yang, and Q. W. Wang, "Experimental investigation of fluid flow and heat transfer in a randomly packed bed of sinter particles," *International Journal of Heat and Mass Transfer*, vol. 99, pp. 589–598, 2016.

[22] B. Eisfeld and K. Schnitzlein, "The influence of confining walls on the pressure drop in packed beds," *Chemical Engineering Science*, vol. 56, no. 14, pp. 4321–4329, 2001.

[23] Z. H. Guo, Z. N. Sun, N. Zhang, and M. Ding, "Influence of confining wall on pressure drop and particle-to-fluid heat transfer in packed beds with small D/d ratios under high Reynolds number," *Chemical Engineering Science*, vol. 209, article 115200, 2019.

[24] J. M. Gorman, A. Zheng, and E. M. Sparrow, "Bounding Wall effects on fluid flow and pressure drop through packed beds of spheres," *Chemical Engineering Journal*, vol. 373, pp. 519–530, 2019.

[25] D. Nemec and J. Levec, "Flow through packed bed reactors: 1. Single-phase flow," *Chemical Engineering Science*, vol. 60, no. 24, pp. 6947–6957, 2005.

[26] E. Ozahi, M. Y. Gundogdu, and M. Ö. Carpinlioglu, "A modification on Ergun's correlation for use in cylindrical packed beds with non-spherical particles," *Advanced Powder Technology*, vol. 19, no. 4, pp. 369–381, 2008.

[27] M. Mayerhofer, J. Govaerts, N. Parmentier, H. Jeanmart, and L. Helsen, "Experimental investigation of pressure drop in packed beds of irregular shaped wood particles," *Powder Technology*, vol. 205, no. 1–3, pp. 30–35, 2011.

[28] K. G. Allen, T. W. V. Backström, and D. G. Kröger, "Packed bed pressure drop dependence on particle shape, size distribution, packing arrangement and roughness," *Powder Technology*, vol. 246, pp. 590–600, 2013.

[29] A. Koekemoer and A. Luckos, "Effect of material type and particle size distribution on pressure drop in packed beds of large particles: extending the Ergun equation," *Fuel*, vol. 158, pp. 232–238, 2015.

[30] J. H. Park, M. Lee, K. Moriyama, M. H. Kim, E. Kim, and H. S. Park, "Adequacy of effective diameter in predicting pressure gradients of air flow through packed beds with particle size distribution," *Annals of Nuclear Energy*, vol. 112, pp. 769–778, 2018.

[31] L. X. Li and W. M. Ma, "Experimental characterization of the effective particle diameter of a particulate bed packed with multi-diameter spheres," *Nuclear Engineering and Design*, vol. 241, no. 5, pp. 1736–1745, 2011.

[32] L. W. Rong, K. J. Dong, and A. B. Yu, "Lattice-Boltzmann simulation of fluid flow through packed beds of spheres: effect of particle size distribution," *Chemical Engineering Science*, vol. 116, pp. 508–523, 2014.

[33] M. Li, Y. T. Mu, J. Y. Zhang, and D. J. Xie, "Numerical simulation and optimization of sinter cooler in multilayered burden distribution," *Journal of Central South University (Science and Technology)*, vol. 44, no. 3, pp. 1228–1234, 2013.

[34] W. Y. Tian, J. Y. Zhang, C. D. Dai, X. H. Zhang, and J. P. Wang, "Segregation feeding on sinter circular cooler," *Journal of Central South University (Science and Technology)*, vol. 46, no. 4, pp. 1182–1188, 2015.

[35] J. C. Leong, K. W. Jin, J. S. Shiau, T. M. Jeng, and C. H. Tai, "Effect of sinter layer porosity distribution on flow and temperature fields in a sinter cooler," *International Journal of Minerals, Metallurgy and Materials*, vol. 16, no. 3, pp. 265–272, 2009.

[36] M. J. Keyser, M. Conradie, M. Coertzen, and J. C. Van Dyk, "Effect of coal particle size distribution on packed bed pressure drop and gas flow distribution," *Fuel*, vol. 85, no. 10–11, pp. 1439–1445, 2006.

[37] S. Z. Zhang, Z. Wen, X. L. Liu, X. Liu, S. Wang, and H. Zhang, "Experimental study on the permeability and resistance characteristics in the packed bed with the multi-size irregular particle applied in the sinter vertical waste heat recovery technology," *Powder Technology*, vol. 384, pp. 304–312, 2021.

[38] S. Z. Zhang, Z. Wen, X. L. Liu, H. Zhang, X. H. Liu, and S. Wang, "Effects of particle shape on permeability and resistance coefficients of sinter packed bed," *Journal of Central South University (Science and Technology)*, vol. 52, no. 4, pp. 1066–1075, 2021.

[39] S. Z. Zhang, Z. Wen, X. L. Liu, H. Zhang, S. Wang, and X. H. Liu, "Gas resistance characteristics in vertical tank with irregular sinter for waste heat recovery," *Journal of Central South University (Science and Technology)*, vol. 52, no. 6, pp. 1963–1973, 2021.

[40] J. S. Feng, H. Dong, H. Z. Li, and J. Y. Gao, "Flow resistance characteristics in vertical tank for sinter waste heat recovery," *Journal of Central South University (Science and Technology)*, vol. 48, no. 4, pp. 867–872, 2017.